

Transcapacitances and Bias Dependent Time Delay and Base Resistance Expressions for Accurate Large Signal Modeling of HBTs

A. Issaoun¹, D. Dousset², A. B. Kouki¹, F. M. Ghannouchi²

¹Ecole de Technologie Supérieure, 1100 Notre-Dame St. W., Montréal, Canada, H3C 1K3

²Ecole Polytechnique de Montréal, P.O. Box 6090, su. Centre-ville, Montréal, Canada, H3C 3A7

Abstract — Transcapacitances and bias dependent total time delay and base resistance expressions for accurate modeling of heterojunction bipolar transistors (HBTs) are proposed. Small-signal equivalent circuit parameters are first extracted over the entire forward bias region using multi-bias S-parameter measurements. Relations taking into account the variation of the bias dependence of circuit elements on collector-emitter voltage and collector current are then developed. The resulting expressions are used to construct a large signal model, which is then tested and compared to a dedicated small-signal model and measurements. The developed expressions may be used to improve the accuracy of other large signal models.

I. INTRODUCTION

Heterojunction bipolar transistors (HBTs) have become very promising devices for future applications at microwave- and millimeter-wave frequencies. A critical requirement for any successful design is the availability of an accurate large-signal model capable of describing the device's behavior over broad bias and frequency ranges. This in turn requires an accurate DC model, on one hand, and to a precise description of the variation of the small-signal intrinsic elements with bias and frequency, on the other hand. Recently, the VBIC model [1] has been developed to be as compatible as possible with the SPICE Gummel-Poon model while overcoming its major DC limitations, [1]-[3]. Hence, the VBIC model satisfies the first requirement but still lacks the description of the bias dependant elements with biasing, which is essential for accurate large-signal modeling. The VBIC limitations were overcome by the UCSD model [4] but at the cost of higher model complexity and a large number of parameters. To date, to the best of the author's knowledge, there is no robust and analytical method capable of extracting directly the small-signal equivalent circuit elements for these two models, over the entire forward bias region, which is required for the study.

In this paper, the new technique for direct extraction of HBT small-signal parameters developed in [5] is used to extract the small-signal equivalent circuit elements, see Fig. 1, over the entire forward bias region. The base-collector (C_{bc}) and base-emitter (C_{be}) junction capacitances as well as the total transit time (τ_d) and distributed base resistance (R_{bb}) are found to be dependent on both collector current and collector voltage. Based on these extracted values, new expressions for modeling these bias dependent elements are developed.

Using these expressions along with the DC model, a large signal model is constructed. To assess the validity of the new expressions, the large signal model is simulated in small-signal mode at various measured bias points. Results of these simulations are compared to measurements and to a dedicated small signal model for an AlGaAs/GaAs transistor of $2 \times 25 \mu\text{m}^2$ emitter area.

II. MODELING EQUATIONS

Fig.1 shows the equivalent circuit diagram of the large-signal model without parasitic elements, as they are bias independent and removed using a de-embedding technique. Values for R_b , R_c and R_e are extracted using the fly-back method. C_{bc} , C_{be} , C_c , R_{bb} and τ_d model the AC parameters of the HBT. Their values are obtained using the extraction procedure detailed in [5].

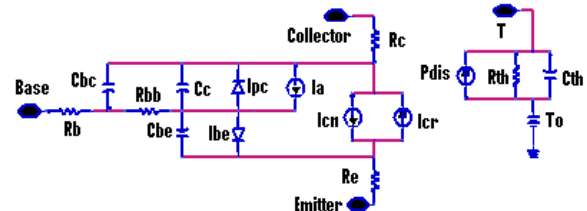


Fig. 1. Equivalent circuit diagram of the large-signal model without parasitic elements

I_{cn} is the electron current injected from the emitter to the base in the forward bias condition. I_{cr} is the electron current injected from the collector to the base in the reverse bias condition. I_{be} is the direct base current representing all recombination processes taking place in the base emitter junction in the forward bias condition. I_{pc} is the base current in reverse bias; hole current injected from the base to the collector sometimes increased by the recombination current in the depletion region. I_a is the Avalanche current. Except for I_a , these currents follow a same type of modeling equations:

$$I = I_{so} e^{\frac{E_{gcn}(T)}{V_t} \left(\frac{T}{T_0} - 1 \right)} \left(\frac{T}{T_0} \right)^X \left(e^{\frac{V_{be}}{N \cdot V_t}} - 1 \right) \quad (1)$$

where T_0 is the absolute reference temperature, I_{so} is the saturation current at T_0 , V_{be} is the applied base emitter potential, X is a temperature coefficient, N is an ideality factor, V_t is the thermal voltage and $E_{gcn}(T)$ defines the

temperature dependence of the band gap energy and finally T is the absolute junction temperature computed by using a self-heating electrical equivalent sub-circuit:

$$T = T_o + R_{th}(T) * P_{diss} \quad (2)$$

where P_{diss} is the total dissipated power in the junction and $R_{th}(T)$ is the thermal resistance at junction temperature T given by:

$$R_{th}(T) = R_{th}(T_o) * (T/T_o)^n \quad (3)$$

Where $R_{th}(T_o)$ is the thermal resistance at the reference temperature T_o .

The base collector capacitance is commonly modeled using the following relation:

$$C_{bc} = C_o \left(1 - \frac{V_{bc}}{V_{jbc}} \right)^{-m} \quad (4)$$

This relation models accurately the variation of the capacitance with respect to base-collector voltage, for a fixed collector current but fails when the collector current is changed. This capacitance does indeed vary with both collector voltage and collector current. So to take into account this variation, expression (4) has been modified to a transcapacitance form:

$$C_{bc} = (x_1 + x_2 I_c) \left(1 - \frac{V_{bc}}{V_{jbc}} \right)^{-m} \quad (5)$$

where V_{jbc} , m , x_1 and x_2 are parameters to be determined using a least-square fitting of equation (5) to the extracted data. Similarly, the inner base-collector capacitance is also modeled in a transcapacitance form as follows:

$$C_c = 10e-14 (x_3 + x_4 I_c) \left(1 - \frac{V_{bc}}{V_{jbc}} \right)^{-m} \quad (6)$$

where V_{jbc} , m , x_3 and x_4 are parameters to be determined using a least-square fitting. The base-emitter diffusion capacitance has been modeled using the following three-parameter equation:

$$C_{be} = C_o [(x_5 + x_6 I_c) * V_{ce}]^{x_7} \quad (7)$$

where x_5 , x_6 and x_7 are parameters to be determined using a least-square fitting. The small-signal time delay, which represents the total transit time involved in the device, is also found to be dependent on both collector current and collector voltage and is modeled by:

$$\tau_d = (x_8 + x_9 I_c) + x_{10} V_{ce} \quad (8)$$

where x_8 , x_9 and x_{10} are parameters to be determined using a least-square fitting. The distributed base resistance, which is crucial for accurate current source modeling, is found to exhibit variation with both collector current and collector voltage and is modeled by:

$$R_{bb} = x_{11} + x_{12} I_c + x_{13} V_{ce} \quad (9)$$

where x_{11} , x_{12} and x_{13} are parameters to be determined using a least-square fitting. It was found that x_{13} is very small and can be neglected.

III. RESULTS AND DISCUSSION

The large-signal shown in Fig. 1 was constructed in HP-ADS simulator using a symbolic defined device (SDD) and tested for $2 \times 25 \mu m^2$ emitter area transistor. The DC parameters used in the simulations are listed in Table I; they were extracted from measured forward and reverse Gummel at different temperatures and I_c - V_{ce} characteristics data. Fig. 2 shows the I_c - V_{ce} curves comparison between the model predictions and the measurements.

Parameter	Value	Parameter	Value
Iscno	3.03 e-24	Xcn	2.17
Iscro	12.4 e-24	Xrsc	9.6
Ispco	3 e-15	Rth(To)	84
Isrsco	1.16 e-23	n	1.24
Npc	1.6225	Egrsco	1.65
Ncn	1.0677	α_e	0.078
Nrsc	1.219	α_{egcn1}	4e-4
Ncr	1.017	α_{egcn2}	150
ϕ_{bc}	0.95	Xk	1.11
α_k	11.58	α_{i2}	0.0019
Egcn0	1.54	I1	0.0178
Re	0.6	Rc	9.4
Rb	5.6		

TABLE I
EXTRACTED DC PARAMETERS AT $T=25^\circ C$.

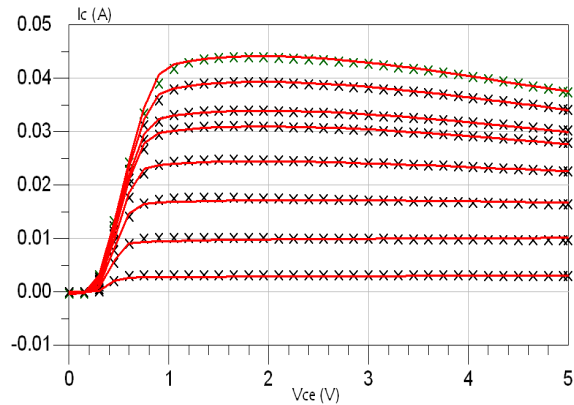


Fig. 2. I_c - V_{ce} curves comparison between model prediction (—) and measurements (x).

The small-signal intrinsic elements are extracted directly over the entire forward bias region using the extraction technique developed in [5]. Tables II and III present the extracted intrinsic element values at 5mA and 15 mA collector currents, respectively, for different collector-emitter voltages. As can be seen from these tables, these parameters exhibit variation with both collector current and voltage. Table IV summarizes the various parameters of equations (5-9), obtained by a least-square fitting. Fig. 3 shows the dependence of C_{bc} on the collector current and the quality of the fitting of

equation (5). Figs. 4, 5 and 6 show s-parameter results obtained using the large signal model used at fixed values as extracted by a dedicated small-signal parameter extraction method, and the large signal model based on the fitting equations (5)-(9), the measured data at $V_{ce}=2.5V$ and for $I_c=5mA$, $I_c=15mA$ and $I_c=30mA$, respectively. In these figures column (c) shows the exact reproduction of the extracted values by the proposed equations (5)-(9). These, as well as other simulation results, indicate the accuracy of the bias dependence equation developed. Fig. 7 shows the input/output power performances of the large-signal compared to measurements, at 2 GHz for a bias condition of $V_{ce}=3V$ and $I_c=20mA$.

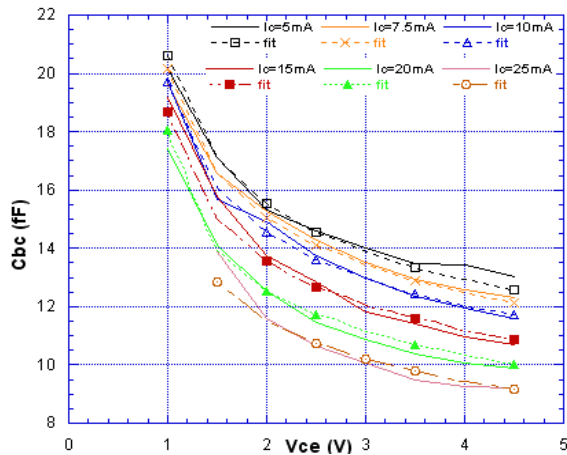


Fig. 3. Extracted and fitted of C_{bc} values.

V_{ce} (V)	C_{be} (pF)	C_{bc} (fF)	C_c (fF)	τ_d (ps)	R_{bb} (Ω)
1.0	0.52	20.15	25.50	0.82	6.23
1.5	0.60	17.09	19.82	1.17	6.4
2.0	0.69	15.30	16.79	1.4	6.5
2.5	0.76	14.58	14.44	1.58	6.7
3.0	0.81	14.01	12.80	1.75	6.9
3.5	0.86	13.48	11.59	1.92	7.0
4.0	0.88	13.45	10.57	2.04	7.3
4.5	0.92	13.04	9.87	2.19	7.4

TABLE II
EXTRACTED INTRINSIC PARAMETERS AT $I_c=5mA$

V_{ce} (V)	C_{be} (pF)	C_{bc} (fF)	C_c (fF)	τ_d (ps)	R_{bb} (Ω)
1.0	1.16	19.19	17.65	0.79	6.11
1.5	1.48	15.77	12.39	1.09	6.19
2.0	1.75	13.73	10.57	1.39	6.1
2.5	1.93	12.83	9.46	1.59	6.2
3.0	2.10	11.82	8.74	1.81	6.2
3.5	2.18	11.41	8.45	1.93	6.4
4.0	2.25	10.98	8.23	2.06	6.5
4.5	2.33	10.68	8.10	2.17	6.6

TABLE III
EXTRACTED INTRINSIC PARAMETERS AT $I_c=15mA$.

C_{bc}		C_c		C_{be}		τ_d		R_{bb}	
Par.	Value	Par.	Value	Par.	Value	Par.	Value	Par.	Value
m	0.2	m	0.54	x_5	-2.66	x_8	0.78	x_{11}	7.04
V_{jbc}	0.69	V_{jbc}	1.087	x_6	1.67	x_9	-0.04	x_{12}	-0.04
x_1	1.879	x_3	2.406	x_7	0.43	x_{10}	0.388		
x_2	-0.02	x_4	-0.07	Fc	0.5	X_{jc}	0.8		

TABLE IV
INTRINSIC ELEMENTS AND THEIR FITTING VALUES

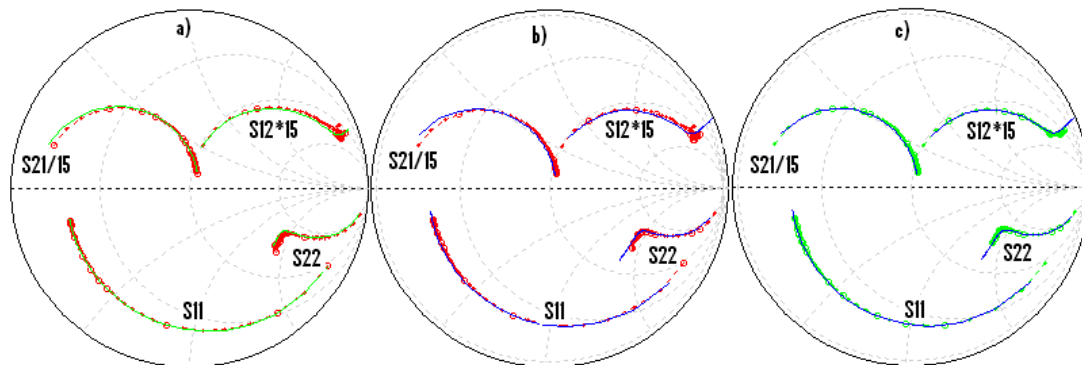


Fig. 4. Small-signal comparisons for a $2*25\mu m^2$ HBT device at $I_c=5mA$, $V_{ce}=2.5V$; over 1 to 30 GHz

- a) Dedicated small signal model (—) and the measurements (---)
- b) Large signal model with fitted equations (—) and measurements (---)
- c) Large signal model with fixed values (—) and large signal model with fitted equations (---)

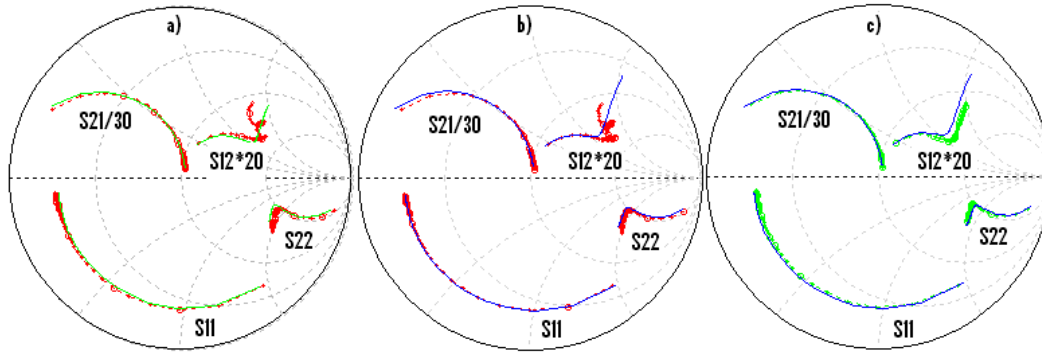


Fig. 5. Small-signal comparisons for a $2 \times 25 \mu\text{m}^2$ HBT device at $I_c=15\text{mA}$, $V_{ce}=2.5\text{V}$; over 1 to 30 GHz
 a) Dedicated small signal model (—) and the measurements (---)
 b) Large signal model with fitted equations (—) and measurements (---)
 c) Large signal model with fixed values (—) and large signal model with fitted equations (—)

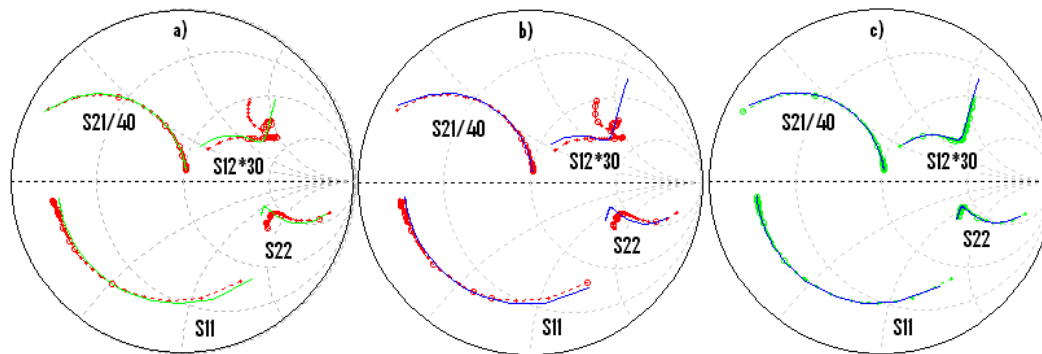


Fig. 6. Small-signal comparisons for a $2 \times 25 \mu\text{m}^2$ HBT device at $I_c=30\text{mA}$, $V_{ce}=2.5\text{V}$; over 1 to 30 GHz
 a) Dedicated small signal model (—) and the measurements (---)
 b) Large signal model with fitted equations (—) and measurements (---)
 c) Large signal model with fixed values (—) and large signal model with fitted equations (—)

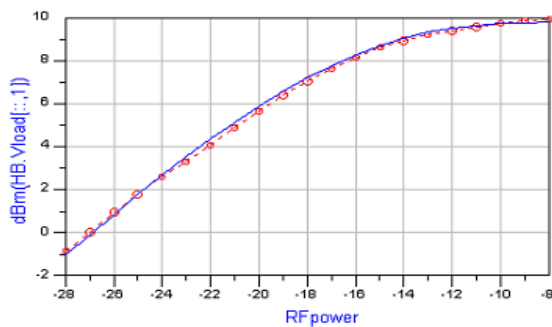


Fig. 7. Measured (o) and modeled (—) microwave power characteristics at 2 GHz for a bias condition of $V_{ce}=3\text{ V}$ and $I_c=20\text{ mA}$.

VI. CONCLUSION

Expressions for modeling bias dependent intrinsic elements of heterojunction bipolar transistors have been developed and presented. The relations take into account the variation of the bias dependent circuit elements on both the collector-emitter voltage and the collector current. The accuracy of these relations over a wide range of bias points and frequencies has been demonstrated through various comparisons. These expressions are crucial for accurate large-signal

predictions of HBT performances. Although these expressions have been tested using a modified Gummel-Poon model; they may also be used to improve the modeling of the bias dependent intrinsic elements of other models that use a similar type of small-signal equivalent circuit, such as the VBIC model.

REFERENCES

- [1] C. C. McAndrew, J. A. Seitchik, D. F. Bowers, M. Dunn, M. Foisy, I. Getreu, M. McSwain, S. Moinian, J. Parker, D. J. Roulston, M. Schroter, P. Wijnen, L. F. Wagner; "VBIC95, the vertical bipolar inter-company model," *IEEE Journal of Sld. Stat. Ckt.*, vol. 31, no. 10, Oct. 1996, pp. 1476–1483.
- [2] C.K. Maiti, B. Senapati, "Advanced SPICE modelling of SiGe HBTs using VBIC model," *IEE Proceedings Circuits, Devices and Systems*, vol. 149 no 2, Apr. 2002, pp. 129-135.
- [3] G.W. Huang, K. M. Chen, J. F. Kuan, Y. M. Deng, S. Y. Wen, D. Y. Chiu, M. T. Wan, "Silicon BJT modeling using VBIC model", *Asia-Pacific Microwave Conference*, Vol. 1, 2001, pp.240–243.
- [4] <http://hbt.ucsd.edu/>
- [5] D. Dousset, A. Issaoun, A. B. Kouki, F. M. Ghannouchi, "A Novel Method for a Direct Extraction of HBT Small-Signal Parameters Using Analytical Expressions," *Asia-Pacific Microwave Conference*, WEOF-15, 2002, pp.374-377.